Periodic Defects in 2D-PBG Materials: Full-Wave Analysis and Design

Fabrizio Frezza, *Senior Member, IEEE*, Lara Pajewski, and Giuseppe Schettini, *Member, IEEE*

***Abstract*—In this paper, an accurate and efficient characterization of two-dimensional photonic bandgap structures with periodic defects is performed, which exploits a full-wave diffraction theory developed for one-dimensional gratings. The high convergence rate of the proposed technique is demonstrated. Results are presented for both TE and TM polarizations, showing the efficiencies as a function of wavelength, incidence angle, geometrical and physical parameters. A comparison with other theoretical results reported in the literature is shown with a good agreement. The transmission properties of photonic crystals with periodic defects are studied, investigating the effects of the variation of geometrical and physical parameters; design efficiency maps and formulas are given; moreover, the application of the analyzed structures as filters is discussed.**

***Index Terms*—Electromagnetic scattering by periodic structures, gratings, microwave filters, passive filters.**

I. Introduction

PHOTONIC BANDGAP (PBG) materials [1] are periodic structures of great interest for their applications both in the microwave region and in the optical range. In PBG structures, periodic implants of material with a specific permittivity are embedded in a homogeneous background of different permittivity; the implants are comparable in size to the operation wavelength, and they may be dielectric or metallic, but also magneto-dielectric, ferromagnetic, ferroelectric, or active. The main feature resulting is the presence of frequency bands within which the waves are highly attenuated and do not propagate [2]. This property is exploited in a lot of electromagnetic and optical applications, such as microwave and millimeter-wave antenna structures, waveguides, planar reflectors, integrated circuits, and more [3]–[5]. The most commonly used methods for the analysis and design of PBG materials are the plane-wave-expansion method [1], the finite-difference method [6], the finite-element method [7], and the transfer-matrix method [8]. Various other methods have been used, such as hybrid ones [9], [10]. It is noted that most PBG applications deal with two-dimensional (2–D) structures, that are invariant along a longitudinal axis and periodic in the transverse plane [6], [11]. A 2–D PBG structure is easier to manufacture than a three-dimensional (3-D) one [12], [13].

The study of photonic crystals with defects is a topic of great interest in the field of PBG materials. Defects may be present in a structure due to fabrication errors. Very often, however, PBG materials with defects are on purpose designed to act as resonant cavities, filters or switches, since the occurrence of a sharp transmission peak in the bandgap results from defect creation. In [14], the properties of a 2-D hexagonal array of air holes in a dielectric material with defects are studied. For what concerns microcavities built into photonic crystals, they allow enhancing the spontaneous emission into the lasing mode and reducing it into the spectrum of the nonlasing modes, so they greatly increase the efficiency of lasers [15], [16]. In [17], measurements of microcavity resonances in PBG structures with defects, directly integrated into a submicrometer-scale silicon waveguide, are reported. The feasibility of optical filters and switches using dielectric PBG structures with periodic defects is investigated in [18]. In [19], a square microstrip resonator, with a PBG structure with defects in the lattice on the ground plane, is used to design a passband filter (also realized and measured). In [20], a dielectric-waveguide filter made of a 2-D PBG structure with defects is designed, realized, and measured. In [21], an electromagnetic bandgap high-Q defect resonator, made of a periodic lattice of vias in a host dielectric substrate with a defect, is used to develop high-quality multipole filters.

The purpose of this paper is to investigate the characteristics of 2-D finite PBG materials with periodic defects, by using a full-wave method for diffraction gratings. In fact, a PBG structure can be considered as a stack of diffraction gratings separated by homogeneous layers, as pointed out in [22] where a S-matrix approach has been employed. With our approach, taking advantage of recent calculation techniques as was done in [23], it is possible to analyze and design, in a stable and rapidly convergent way, electromagnetic crystals with rods having an arbitrary shape; the rods can form rectangular, triangular, hexagonal, or whatever kind of lattice, and they can be made of isotropic or anisotropic dielectric as well as of metallic material. Several kinds of periodic defects can be considered: some layers of rods can be missing, or somehow different in shape and material from the other ones, or else not perfectly aligned.

In Section II, we explain how a rigorous diffraction theory for multilevel gratings can be used to model and characterize 2D-PBG materials with periodic defects. We briefly resume the formulation of the employed full-wave theory and discuss the potentiality of such a method.

In Section III, we first check the efficiency and accuracy of the approach and numerical implementation that we have developed: convergence figures as well as comparisons with theoretical results taken from the literature, are reported and commented on. Then, a detailed study of PBG materials made of di-

Manuscript received January 30, 2003; revised March 22, 2003.

F. Frezza and L. Pajewski are with the Department of Electronic Engineering, "La Sapienza" University of Rome, 00184 Rome, Italy (e-mail: fabrizio.frezza@uniroma1.it).

G. Schettini is with the Department of Applied Electronics, Rome Tre University of Rome, 00146 Rome, Italy (e-mail: g.schettini@uniroma3.it).

Digital Object Identifier 10.1109/TNANO.2003.817227

1536-125X/03$17.00 © 2003 IEEE

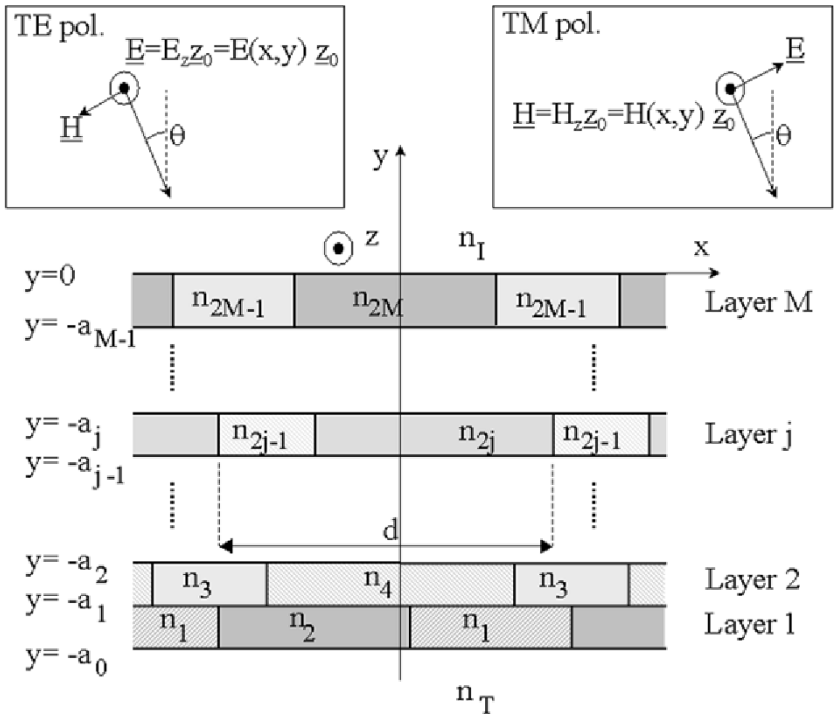

Fig. 1. Geometry of a multilevel grating.

electric parallel rods with a rectangular section, with a periodic defect consisting of a central layer of rods with different shape and permittivity, is presented. We investigate the effects of the variation of geometrical and physical parameters on the transmission properties of such a structure, and we give efficiency maps and design formulas. Moreover, we discuss the applicability of this kind of PBG materials with periodic defects as frequency and polarization selective filter.

In Section IV, concluding remarks are finally given.

II. Characterization of 2-D-PBG Materials by Use of a Full-Wave Theory for Gratings

A 2-D electromagnetic crystal may be considered as a stack of periodic grids of rods separated by homogeneous layers, i.e., as a stack of one-dimensional diffraction grating. As a consequence, it is clear that 2-D-PBG materials can be analyzed and designed by using a rigorous diffraction theory for multilevel gratings.

The formulation of the full-wave theory that we employ is described in [23]. In short, consider a monochromatic plane wave of wavelength λ (in a vacuum), impinging at an angle ϑ on the multilevel grating of period d shown in Fig. 1. The typical layer j ($1 \leq j \leq M$, where M is the number of layers) is a binary grating including several alternate regions of refractive indices n_{2j-1} and n_{2j}, respectively. The multilevel grating ($-a_0 < y < 0$) is bounded by two possibly different media having refractive indices n_I and n_T, respectively. As is known, the incident polarization may be decomposed into the two fundamental TE (electric field parallel to the grating grooves) and TM (magnetic field parallel to the grating grooves) polarizations (see the insets in Fig. 1). The general approach for exactly solving the electromagnetic problem associated with the diffraction grating involves the solution of Maxwell's equations in each of the $M + 2$ following regions: the incidence region, the M grating layers, and the transmission region. Since the refractive index of the jth layer of the grating, say $n_j(x)$, is a periodic function, its square can be expanded in a Fourier series. Such a Fourier decomposition of the permittivity function, together with a planewave expansion of the electromagnetic fields (Rayleigh expansions in incidence and transmission regions, modal expansions in grating layers), leads to an eigenvalue problem which has to be solved in each grating layer. Then, the tangential electric and magnetic field components have to be matched at all the boundary surfaces. The resulting equation system is to be solved for the reflected and transmitted field amplitudes, so that the diffraction efficiencies can be determined.

To obtain a high convergence rate even in TM polarization, we used the formulation of the eigenvalue problem presented in [24] and [25]. To overcome numerical problems due to ill-conditioned matrices obtained on imposing the boundary conditions, and to improve numerical stability and efficiency of the implemented codes, we applied the technique presented in [26] to both polarizations.

The above-summarized full-wave theory provides a solution of the problem of electromagnetic diffraction by grating structures to an arbitrary degree of accuracy [27].

Our treatment of the PBG structures is very versatile, since it allows us to study electromagnetic crystals with rods having an arbitrary shape [see Fig. 2(a)]; moreover, the rods can form whatever kind of lattice, as sketched in Fig. 2(b). Of course, also PBG materials made of holes in a host medium, instead of rods, may be studied.

As pointed out in the Introduction, with our approach photonic bandgap materials with periodic defects can be studied.

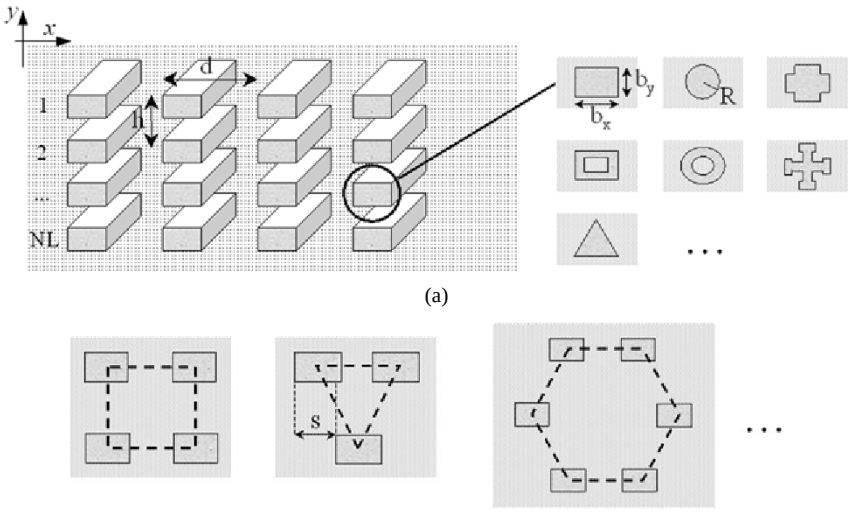

Fig. 2. (a) With the described approach, it is possible to study electromagnetic crystals with rods having an arbitrary shape. (b) The rods can form rectangular, triangular, hexagonal, or whatever kind of lattice.

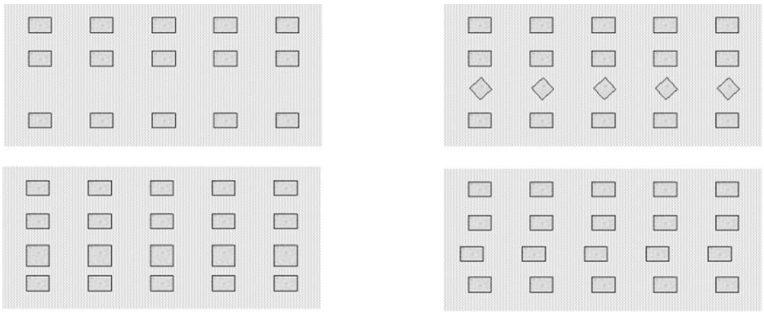

Fig. 3. Presence of periodic defects, which can be taken into account with our approach.

For example, PBG structures in which some layers of rods (as well as layers of the homogeneous background) are missing may be characterized. Moreover, the presence of rods with a shape somehow different from the other ones, as well as the occurrence of layers not perfectly aligned, may be taken into account. A few possible defects are sketched in Fig. 3 for the simplest case of a PBG material made of rectangular parallel rods forming a rectangular lattice.

III. Numerical Results

In order to check the efficiency and accuracy of our approach and numerical implementation, in this section we compare our numerical results with other presented in the literature; we also report and comment on some convergence data (Section III-A). Then, we consider 2-D square-lattice square-section-rod PBG materials with periodic defects, and study their transmission properties, investigating the effects of the variation of geometrical and physical parameters; we give efficiency maps and design formulas, and discuss the application of such structures as filters (Section III-B).

We now introduce some symbols that are used throughout this section. With reference to a PBG structure without defect (see Fig. 2): b_x and b_y are the dimensions, along x and y respectively, of a rectangular-section rod; d and h are the periods, along x and y, respectively, of the electromagnetic crystal. In a triangular lattice, we assume that there is a lateral shift s between two neighboring layers of rods, so that s can vary from 0 (when the triangular lattice degenerates in a rectangular one) to $0.5d$. For each geometrical configuration, it is customary to define the so-called filling factor F, which represents the fraction of the unit cell of the periodic structure filled by the rod. The parameter NL represents the number of rod layers in the finite PBG structure. For what concerns the involved materials, n_r and n_b are the refractive indices of rod and background media, respectively.

As pointed out in Section I, PBG materials with various periodic defects can be studied by using the present method: for example, structures in which some layers of rods are missing, or are somehow different in size or shape from the other ones, or else are not perfectly aligned. In the case presented in Section III-B, the periodic defect consists of a matter excess (see Fig. 4): in the middle of a structure made of an odd number of layers, the central layer has an anomalous thickness b_{yd}, larger than b_y. We use the symbol n_d to denote the refractive index of the central layer, that can in general be different from n_r. We call ND the number of layers located on each side of the central defect, so that $ND = (NL - 1)/2$. The structure can also be viewed as a Fabry–Perot resonator, with the mirrors consisting of the PBG material located on the two sides of the defect.

For what concerns the computational effort, $2N + 1$ is the number of diffraction orders taken into account. Moreover, we

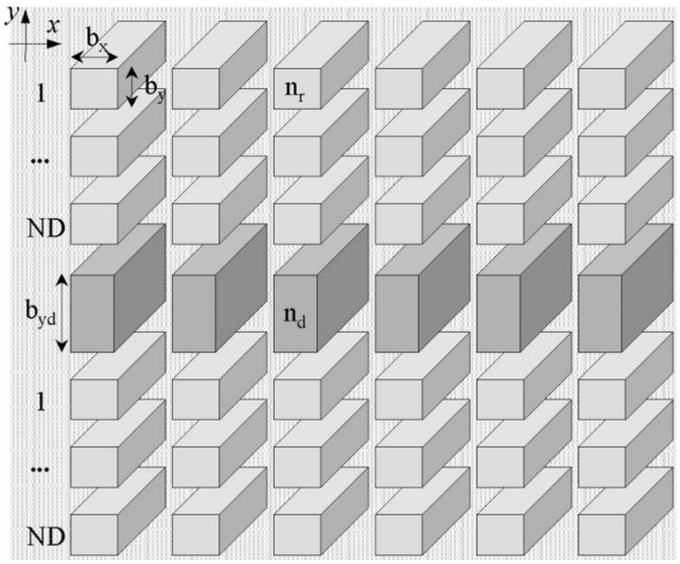

Fig. 4. PBG material with a periodic defect consisting of a matter excess in the middle of the structure.

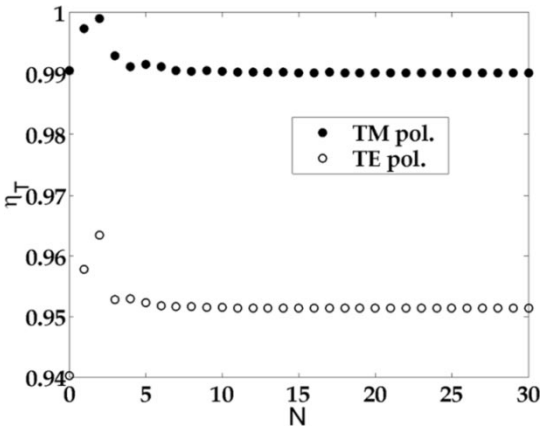

Fig. 5. Convergence of the transmission efficiency η_T as a function of N, for a PBG structure made of a stack of $NL = 15$ layers of rods with a square section: $d = h = 0.7\lambda$, $b_x = b_y = 0.5d$, $b_{yd} = 3b_y$, $n_r = 2$, $n_d = 2.4$, $n_b = 1$.

denote with η_T the total transmission efficiency of the PBG structure, that is the sum of the efficiencies of all the transmitted orders (the efficiency of the nth transmitted order is the ratio between the Poynting-vector y-component of the nth order transmitted wave and that of the incident wave). Analogously, we denote with η_R the total reflection efficiency. Unless otherwise specified, the incident planewave is supposed to impinge normally on the structure ($\theta = 0$). From a practical point of view, due to the finiteness of the structure, it is useful to establish a conventional upper limit for the efficiency value within a stopband: in our case, we arbitrarily assumed the presence of a bandgap when $\eta_T < 0.001$.

A. Convergence, Stability, and Accuracy of Our Approach

An example of the convergence of the results, as a function of N, is shown in Fig. 5 for a PBG structure with a periodic defect, with $NL = 15$ layers (i.e., $M = 30$ and $ND = 7$), made of rods with a square section: $d = h = 0.7\lambda$, $b_x = b_y = 0.5d$, $b_{yd} = 3b_y$. The rod refractive index is $n_r = 2$, the defect index is $n_d = 2.4$ and the host medium is supposed to be a vacuum ($n_b = 1$). From Fig. 5 it is seen that the convergence is very fast; moreover, it can be appreciated that, by using the formulation presented in [24] and [25], we obtain for TM polarization (dots) a rate of convergence similar to the TE polarization one (circles). With $N = 10$, convergence to the third decimal figure is obtained in both polarization cases. With $N = 14$ and $N = 19$, η_T assumes a value which is exact within the fourth decimal figure in TE and TM polarization, respectively.

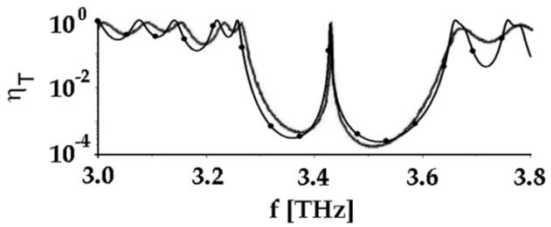

Fig. 6. Comparison between the results obtained by Bastonero *et al.* [28] (solid line) and our results (solid line with dots), for a PBG structure of dielectric square-section rods forming a square lattice, with a central defect: $d = 0.336\ \mu$m, $h = d\sqrt{3}/2$, $b_x = b_y = 0.261\ \mu$m, $s = 0.5d$, $n_r = 1$, $n_b = 3.68$, $b_{yd} = 0.68\ \mu$m, $n_d = n_r$, and $ND = 6$. The transmission efficiency η_T is shown as a function of the frequency f, for TE polarization, when $\theta = 0°$.

To check our codes we made a comparison with the results obtained by Bastonero *et al.* in [28], where a PBG microcavity, built in a dielectric periodic structure of air holes arranged in an equilateral triangular lattice into a bulk semiconductor, is studied. The central row of holes is increased, creating a defect in the crystal, so that a localized resonance mode takes place and it can be used as the laser mode. The whole resonator may be schematized as the structure in Fig. 4, with $d = 0.336\ \mu$m, $h = d\sqrt{3}/2$, $b_x = b_y = 0.261\ \mu$m (which results in a filling factor $F = 0.7$), $s = 0.5d$, $n_r = 1$, $n_b = 3.68$, $b_{yd} = 0.68\ \mu$m, $n_d = n_r$, and $ND = 6$. The transmission response of the entire resonator is shown in Fig. 6, where η_T is plotted as a function of the frequency f (in terahertz); the polarization is TE and $\theta = 0°$. Our results (solid line with dots) can be directly compared with the results of Fig. 6 in [28] (solid line). In particular, in [28] the authors found that the transmission peak for $\theta = 0$ was centered on $f = 343.2$ THz and with our codes we found exactly the same value.

B. 2-D Square-Lattice Square-Rod PBG Materials With Defects

In this section, we consider 2-D square-lattice square-rod PBG materials with periodic defects, and study their transmission properties by use of the approach outlined in Section II. As pointed out in Section I, defects may be present in an electromagnetic crystal due to fabrication errors. Moreover, since the occurrence of sharp transmission peaks in the photonic stopbands results from defect creation, very often PBG materials with defects are on purpose designed to act as frequency and polarization selective filters or switches, or they are employed in the realization of resonators and cavities.

In Fig. 7, the transmission efficiency η_T (full line) is shown as a function of the normalized wavelength λ/d, for a structure with $d = h$, $b_x = b_y = 0.4d$, $n_r = 3.6$, $n_b = 1$, $b_{yd} = 3b_y$, $n_d = n_r$, and $ND = 5$ (so that $NL = 11$); both

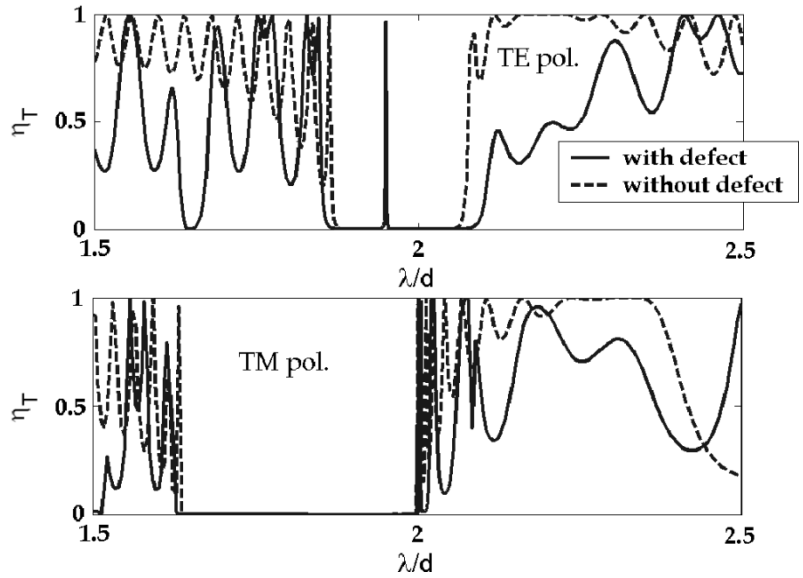

Fig. 7. Transmission efficiency η_T (full line) vs. the normalized wavelength λ/d, for a structure with $d = h$, $b_x = b_y = 0.4d$, $n_r = 3.6$, $n_b = 1$, $b_{yd} = 3b_y$, $n_d = n_r$, and $ND = 5$; both polarization cases are considered; the behavior of the corresponding structure without the defect is also shown (dashed line), for comparison.

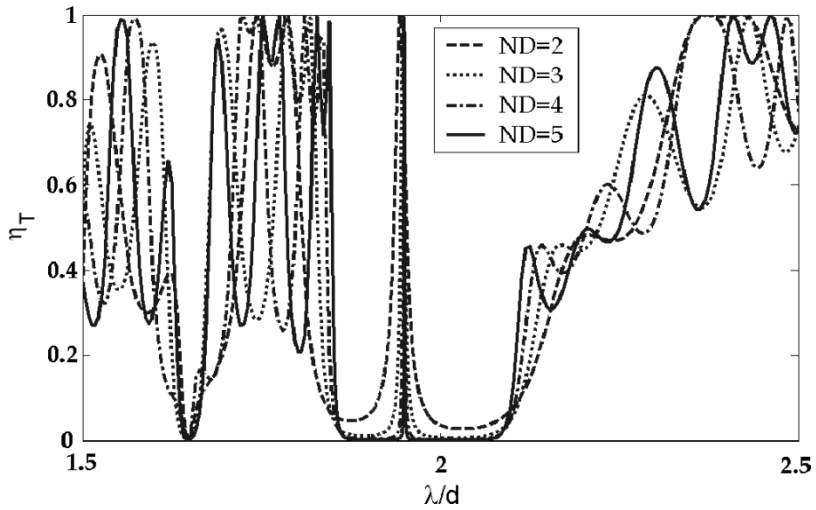

Fig. 8. Transmission efficiency η_T vs. λ/d, for the same structure as in Fig. 7 and for different values of ND; the polarization is TE.

polarization cases are considered. In the same figure, the behavior of the corresponding structure without the defect is also shown (dashed line), for comparison. We have chosen this example because of the existence of a complete bandgap in the $1.89 \leq \lambda/d \leq 2$ range (as is known, if bandgaps for both TE and TM polarization states are present and they overlap each other, then their intersections are called *complete* bandgaps [1]). Looking at Fig. 7, it can be noted, inside the TE stopband, the presence of a sharp transmission peak centered on $\Lambda_c \cong 1.95$, where $\Lambda = \lambda/d$: this is due to the introduction of the defect, and its 3-dB width is $\Delta\Lambda \cong 8 \cdot 10^{-4}$; at the same time, forbidden propagation is kept for TM polarization. Therefore, it is apparent that, by introducing a periodic defect in a PBG material and taking advantage of complete bandgaps, it is possible to realize a narrow-band filter for a particular polarization, while keeping forbidden propagation for the other polarization: the numerical example of Fig. 7 shows that the characteristics of such a kind of frequency- and polarization-selective filters can be easily and precisely modeled with our approach.

We will now discuss how to modify the selectivity of the filter, showing the influence of some key physical and geometrical parameters on the performances of the structure: the number of rod layers located on each side of the defects ND, the defect refractive index n_d, the defect layer thickness b_{yd}, and the incidence angle θ.

In Fig. 8, η_T is shown as a function of λ/d, for the same structure as in Fig. 7 and for different values of ND; the polarization is TE. It is apparent that the selectivity of the filter depends on the number of rod layers located on each side of the defects: the larger ND, the narrower the filter passband, in fact the 3-dB width of the peak is $\Delta\Lambda \cong 1.8 \cdot 10^{-2}$, $6 \cdot 10^{-3}$, and $2.5 \cdot 10^{-3}$, when $ND = 2$, 3, and 4, respectively.

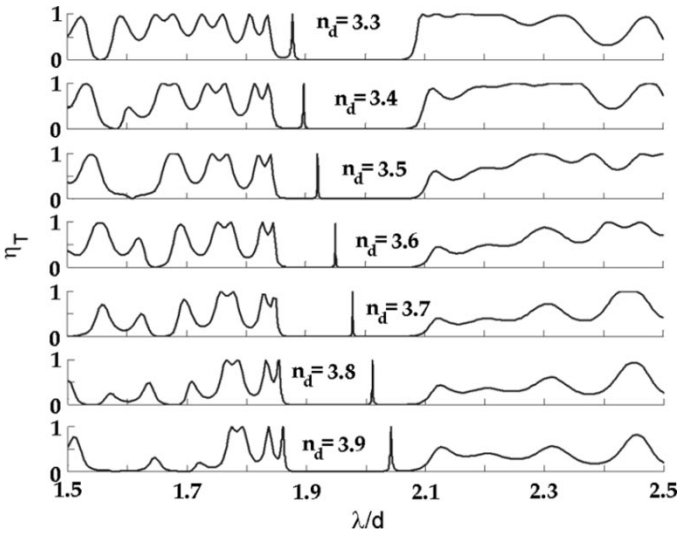

Fig. 9. Transmission efficiency η_T vs. λ/d, for the same structure as in Fig. 7 and for different values of n_d; the polarization is TE.

In Fig. 9, η_T is shown as a function of λ/d, for the same structure as in Fig. 7 and for different values of n_d; the polarization is TE. It is seen that the central wavelength of the peak of the passband filter is highly sensitive to the defect refractive index: with a higher value of n_d, the peak shifts toward larger values of λ/d. It can be also noted that a higher value of n_d causes a reduction of the global transmittance (i.e., of the transmission for the frequencies outside the stopband) of the structure. The influence of the refractive index of the defect on the position of the peak can also be appreciated from the efficiency map reported in Fig. 10(a), where η_T is shown as a function of λ/d and n_d. The gray scale of the map ranges from black ($\eta_T = 0$) to white ($\eta_T = 1$), so that a black region shows the location of a stopband while a white region corresponds to a high transmittance. In Fig. 10(b), an enlargement of Fig. 10(a) is reported, where the wavelength shift of the peak that results from a change of n_d can be appreciated with more evidence.

The movement of the transmission peak inside the bandgap with varying the refractive index of the defect can be described using a Fabry–Perot model. In a Fabry–Perot resonator made of two identical mirrors with an equivalent separation width $L_{\rm eq}$, if f_L is the central frequency of the transmission peak, c is the light velocity in a vacuum, and Φ is the phase of the mirror reflection coefficient, the resonant condition is satisfied when

$$\frac{2\pi f_L L_{\rm eq}}{c} + \Phi = m\pi \quad (m = 0, \pm 1, \pm 2, \ldots) \qquad (1)$$

where in our case $L_{\rm eq} = h - b_y + b_{yd} n_d$ [see Figs. 2(a) and 4]. Increasing the refractive index n_d of the defect makes larger the equivalent length of the cavity $L_{\rm eq}$: from (1) it can be seen that with a higher value of $L_{\rm eq}$ the defect frequency f_L is lower, and therefore the transmission peak has to occur at higher λ values, as in Fig. 9.

In Figs. 11 and 12, the same parameters as in Figs. 9 and 10(a), respectively, are shown for the case of TM polarization: it is seen that a change of n_d does not sensitively affect the location and the amplitude of the stopband, and no transmission peak

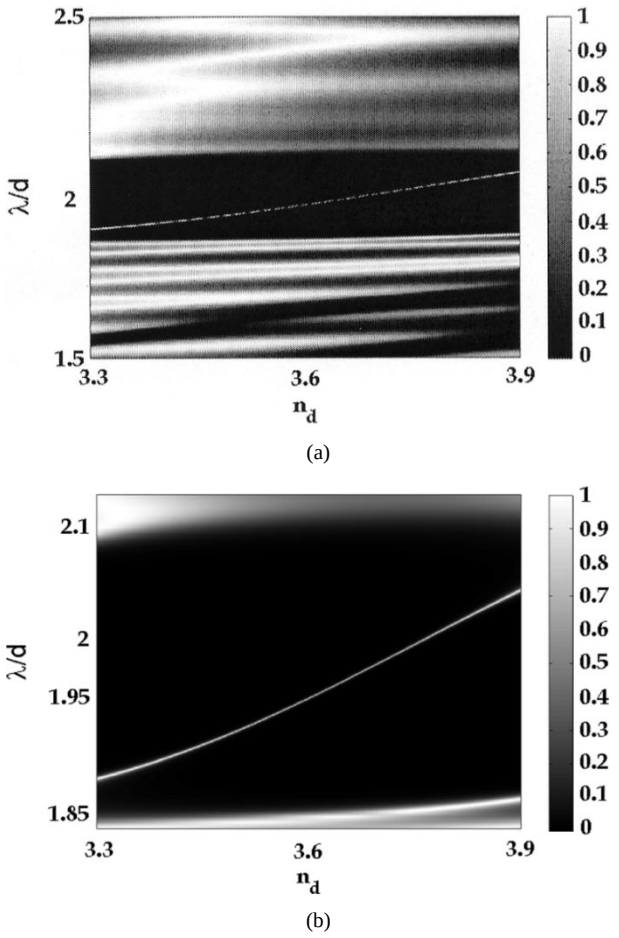

Fig. 10. (a) Gray-scale map of η_T versus λ/d and n_d, for the same structure of Fig. 7, the polarization is TE. (b) An enlargement of (a).

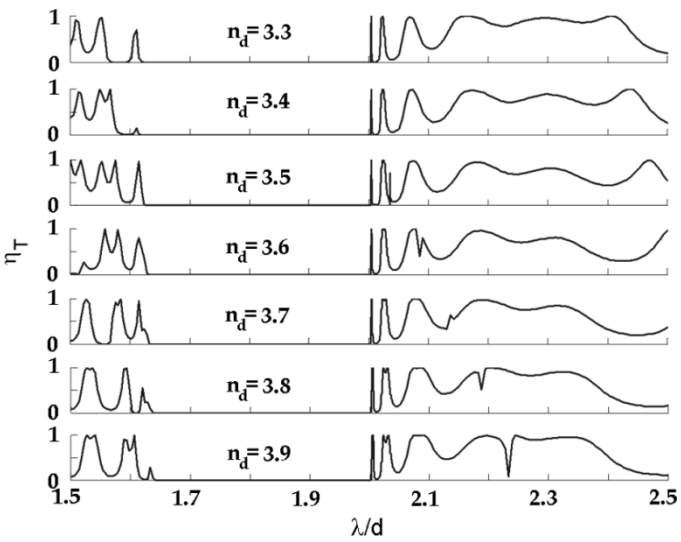

Fig. 11. Transmission efficiency η_T versusλ/d, for the same structure as in Fig. 7 and for different values of n_d; the polarization is TM.

appears. Finally, comparing Figs. 9 and 11, it is worth noting that for $n_d = 3.8$ and $n_d = 3.9$ the TE peak is located outside the complete bandgap.

Fig. 10 can be very useful for determining the value of the defect refractive index needed for positioning the transmission

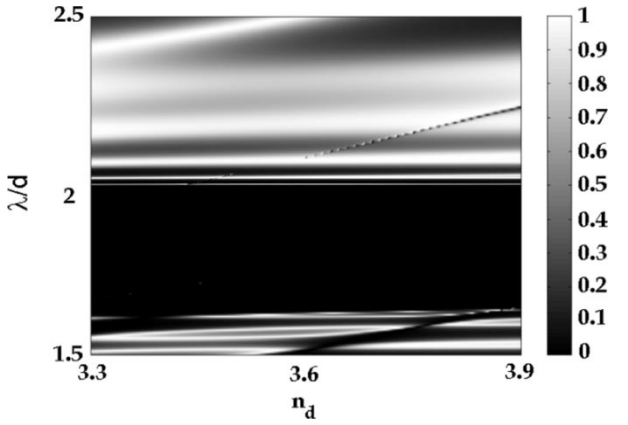

Fig. 12. Gray-scale map of η_T versusλ/d and n_d, for the same structure as in Fig. 7, the polarization is TM.

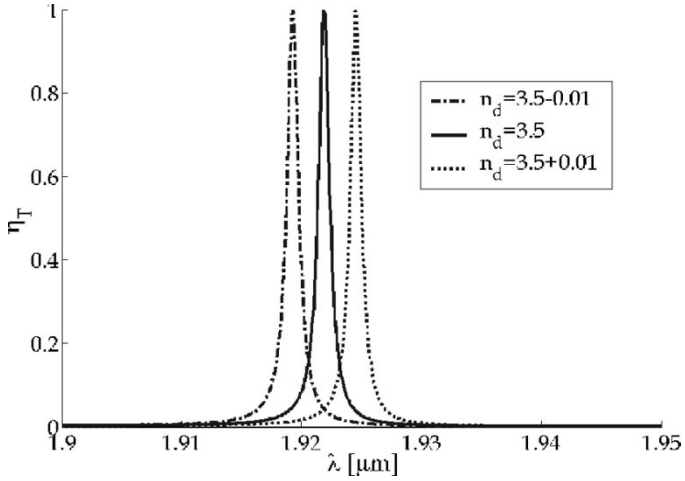

Fig. 13. Transmission efficiency η_T as a function of λ (in μm), for a structure with $d = h = 1\,\mu\text{m}$, $b_x = b_y = 0.4\,\mu\text{m}$, $n_r = 3.6$, $n_b = 1$, $b_{yd} = 3b_y$, $n_d = 3.5$, and $ND = 5$: the wavelength shift of the peak that results from a ± 0.01 change of the defect refractive index is shown; the polarization is TE.

peak central wavelength. However, it can be useful to have at one's disposal a design formula, i.e., a simple expression giving the wavelength position of the peak as a function of the defect refractive index. To this aim, we made a polinomial curve fitting of our numerical results: the coefficients of the polynomials are chosen fitting the data in a least-square sense; the degree of the polynomials is 3 (so that the design formula comes out very simple), and the order of magnitude of the relative error committed in the fitting is 10^{-4}. In the following expression, the normalized central wavelength of the transmission peak Λ_c is given as a function of n_d:

$$\Lambda_c \cong -0.2589\, n_d^3 + 2.9303\, n_d^2 - 10.7361\, n_d + 14.7007. \quad (2)$$

The high sensitivity of the TE-peak central-wavelength to the defect refractive index is shown in Fig. 13, where η_T is reported as a function of λ in μm for a structure with $d = h = 1\ \mu\text{m}$, $b_x = b_y = 0.4\ \mu\text{m}$, $n_r = 3.6$, $n_b = 1$, $b_{yd} = 3b_y$, $n_d = 3.5$, and $ND = 5$: the wavelength shift of the peak that results from a ± 0.01 change of the defect refractive index is apparent.

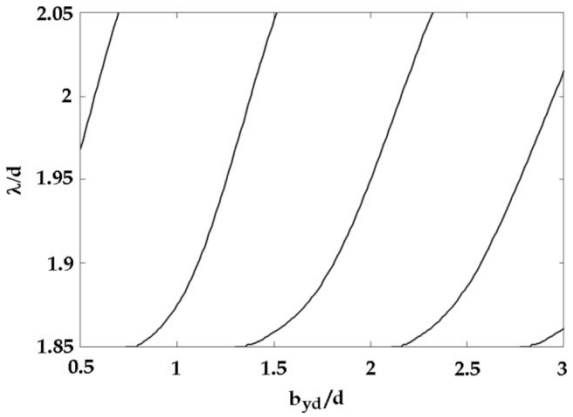

Fig. 14. Central wavelength of the transmission peaks as a function of λ/d and of b_{yd}/d, for the same structure as in Fig. 7; the polarization is TE.

In Fig. 14, the transmission peaks ($\eta_T \cong 1$) vs. b_{yd}/d and λ/d are shown for the same structure as in Fig. 7 and for TE polarization. The central wavelength of the transmission peak Λ_c is seen to be highly sensitive to the defect thickness b_{yd}: in particular, the transmission peak shifts toward higher values of λ when b_{yd} is increased, as predicted by (1) for a Fabry–Perot resonator with a larger equivalent cavity length L_{eq}. Moreover, it can be noted that in correspondence of certain values of b_{yd} our graph suggests that there are two transmission peaks within the bandgap: it implies that a single defect is causing two localized states within the stopband. In particular, this occurs when $1.30 \le b_{yd}/d \le 1.53$, $2.11 \le b_{yd}/d \le 2.36$, and $b_{yd}/d \ge 2.77$ in the considered range: in all these intervals, as the thickness b_{yd} is increased, the peak disappears from the upper edge of the stopband only after the appearance of a second peak from the lower edge of the stopband. This phenomenon could be related to the behavior af a Fabry–Perot under similar conditions (see, for example, [29], where a double-peak formation, analogous to the one here noticed, has been predicted and measured for a photonic crystal with a single defect): since the phase of the mirror reflection coefficient Φ varies with frequency, the difference between the values of Φ at a wavelength closer to the lower edge of the stopband and at a wavelength closer to the upper edge may be high. Therefore, for sufficiently high values of b_{yd}, the resonance condition can be satisfied at two different frequencies, whereas for lower values only one peak is present. This is apparent from Fig. 14, where it can be noted that for lower b_{yd}/d there is no overlapping between the various branches, while the overlapping region occurs larger for higher b_{yd}/d values.

Finally, we analyze the behavior of the PBG structure as a function of the incidence angle θ. To this aim, in Fig. 15 we report η_T vs. θ, for the same structure of Fig. 7 and for different values of n_d, in correspondence with the transmission peak, for both polarization cases. It is seen that, when the polarization is TM, η_T remains negligible for a very large angular range; moreover, it can be noted that, in TE polarization, the angular transmission peak is narrower for higher values of n_d. In fact, as the incidence angle varies, a shift of the central wavelength of the peak occurs.

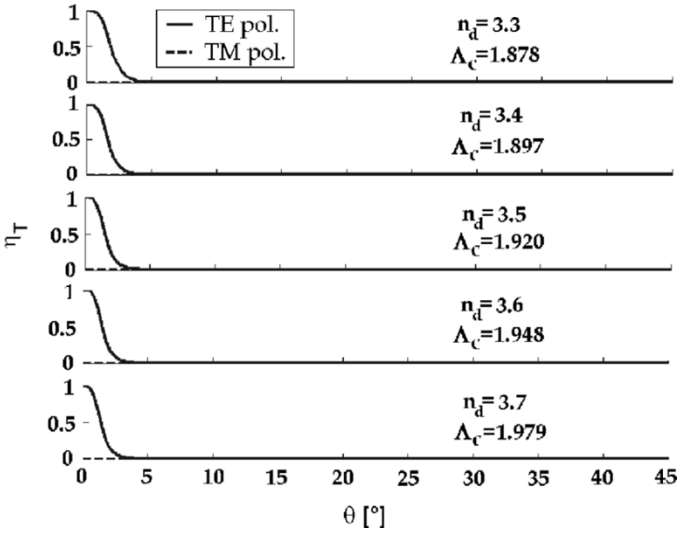

Fig. 15. Transmission efficiency η_T versus the incidence angle θ, for the same structure as in Fig. 7 and for different values of n_d, in correspondence of the TE-transmission peak, for both polarization cases (full line: TE polarization; dashed line: TM polarization).

IV. Conclusions

In this paper, a comprehensive analysis of periodic defects in two dimensional finite thickness, photonic bandgap materials has been presented. A full-wave approach originally developed for diffraction gratings has been exploited with very good results. Both TE and TM polarizations for the incident field have been considered. Curves have been shown to prove the very efficient convergence for both polarizations: in particular, for the TM case suitable acceleration techniques have been adopted. The transmission efficiency has been investigated as a function of frequency and of the geometrical and physical parameters, as well as the incidence angle. The effects of the presence of defects of different nature on the filtering properties have been enlightened, both in frequency and in polarization. Gray-scale maps and an approximate formula, useful in the design procedure to localize the position of the transmission peaks, are reported. A comparison with another result shown in the literature is presented with a good agreement.

References

[1] J. D. Joannopoulos, R. D. Meade, and J. N. Winn, *Photonic Crystals: Molding the Flow of Light*. Princeton, NJ: Princeton Univ. Press, 1995.

[2] E. Yablonovitch, "Inhibited spontaneous emission in solid-state physics and electronics," *Phys. Rev. Lett.*, vol. 58, pp. 2059–2062, May 1987.

[3] R. Coccioli, F.-R. Yang, K.-P. Ma, and T. Itoh, "Aperture-coupled patch antenna on UC-PBG substrate," *IEEE Trans. Microwave Theory Tech.*, vol. 47, pp. 2123–2130, Nov. 1999.

[4] J. G. Maloney, M. P. Kesler, B. L. Shirley, and G. S. Smith, "A simple description for waveguiding in photonic bandgap materials," *Microwave and Opt. Technol. Lett.*, vol. 14, pp. 261–266, Apr. 1997.

[5] M. P. Kesler, J. G. Maloney, B. L. Shirley, and G. S. Smith, "Antenna design with the use of photonic bandgap materials as all-dielectric planar reflectors," *Microwave and Opt. Technol. Lett.*, vol. 11, pp. 169–174, Mar. 1996.

[6] H. Y. D. Yang, "Finite difference analysis of 2-D photonic crystals," *IEEE Trans. Microwave Theory Tech.*, vol. 44, pp. 2688–2695, Dec. 1996.

[7] R. Coccioli, T. Itoh, and G. Pelosi, "A finite element-generalized network analysis of finite thickness photonic crystals," in *IEEE MTT-S International Microwave Symposium Digest*, June 1997, pp. 195–198.

[8] J. B. Pendry, "Photonic structures," *J. Mod. Opt.*, vol. 41, pp. 209–229, Feb. 1994.

[9] S. D. Gedney, J. F. Lee, and R. Mittra, "A combined FEM/MoM approach to analyze the plane wave diffraction by arbitrary gratings," *IEEE Trans. Antennas Propagat.*, vol. 40, pp. 363–370, Feb. 1992.

[10] E. W. Lucas and T. P. Fontana, "A 3-D hybrid finite element/boundary element method for the unified radiation and scattering analysis of general infinite periodic arrays," *IEEE Trans. Antennas Propagat.*, vol. 43, pp. 145–153, Feb. 1995.

[11] M. Sarnowski, T. Vaupel, V. Hansen, E. Kreysa, and H. P. Gemuend, "Characterization of diffraction anomalies in 2-D photonic bandgap structures," *IEEE Trans. Microwave Theory Tech.*, vol. 49, pp. 1868–1872, Oct. 2001.

[12] S. Y. Lin, G. Arjavalingam, and W. M. Robertson, "Investigation of absolute photonic bandgaps in 2-dimensional dielectric structures," *J. Mod. Opt.*, vol. 41, pp. 385–393, Feb. 1994.

[13] J. B. Nielsen, T. Søndergaard, S. E. Barkou, A. Bjarklev, J. Broeng, and M. B. Nielsen, "Two-dimensional kagomé structure, fundamental hexagonal photonic crystal configuration," *Electron. Lett.*, vol. 35, pp. 1736–1737, Sept. 1999.

[14] A. L. Reynolds, U. Peschel, F. Lederer, P. J. Roberts, T. F. Krauss, and P. J. I. de Maagt, "Coupled defects in photonic crystals," *IEEE Trans. Microwave Theory Tech.*, vol. 49, pp. 1860–1867, Oct. 2001.

[15] S. Noda, A. Chutinan, and M. Imada, "Trapping and emission of photons by a single defect in a photonic bandgap structure," *Nature*, vol. 407, pp. 608–610, Oct. 2000.

[16] S. Y. Lin, V. M. Hietala, and S. K. Lyo, "Photonic band gap quantum well and quantum box structures: A high-Q resonant cavity," *Appl. Phys. Lett.*, vol. 68, pp. 3233–3235, June 1996.

[17] J. S. Foresi, P. R. Villeneuve, J. Ferrera, E. R. Thoen, G. Steinmeyer, S. Fan, J. D. Joannopoulos, L. C. Kimerling, H. I. Smith, and E. P. Ippen, "Photonic-bandgap microcavities in optical waveguides," *Nature*, vol. 390, pp. 143–145, Nov. 1997.

[18] P. Dansas, N. A. Paraire, and S. Laval, "Feasibility of optical filters and switches using plastic photonic bandgap structures," *SPIE Proceedings*, vol. 3135, pp. 219–229, July 1997.

[19] S. T. Chew and T. Itoh, "PBG-excited split-mode resonator bandpass filter," *IEEE Microwave and Wireless Components Lett.*, vol. 11, pp. 364–366, Sept. 2001.

[20] C.-Y. Chang and W.-C. Hsu, "Photonic bandgap dielectric waveguide filter," *IEEE Microwave Wireless Components Lett.*, vol. 12, pp. 137–139, Apr. 2002.

[21] W. J. Chappell, M. P. Little, and L. P. B. Katehi, "High isolation, planar filters using EBG substrates," *IEEE Microwave and Wireless Components Lett.*, vol. 11, pp. 246–248, June 2001.

[22] P. Dansas and N. Paraire, "Fast modeling of photonic bandgap structures by use of a diffraction-grating approach," *J. Opt. Soc. Am. A*, vol. 15, pp. 1586–1598, June 1998.

[23] R. Borghi, F. Frezza, L. Pajewski, M. Santarsiero, and G. Schettini, "Full-wave analysis of the optimum triplicator," *J. of Electromagn. Waves and Appl.*, vol. 15, pp. 689–707, May 2001.

[24] P. Lalanne and G. M. Morris, "Highly improved convergence of the coupled-wave method for TM polarization," *J. Opt. Soc. Am. A*, vol. 13, pp. 779–784, Apr. 1996.

[25] G. Granet and B. Guizal, "Efficient implementation of the coupled-wave method for metallic lamellar gratings in TM polarization," *J. Opt. Soc. Am. A*, vol. 13, pp. 1019–1023, May 1996.

[26] M. G. Moharam, D. A. Pommet, E. B. Grann, and T. K. Gaylord, "Stable implementation of the rigorous coupled-wave analysis for surface-relief gratings: Enhanced transmittance matrix approach," *J. Opt. Soc. Am. A*, vol. 12, pp. 1077–1086, May 1995.

[27] L. Li, "Justification of matrix truncation in the modal methods of diffraction gratings," *Pure Appl. Opt.*, vol. 1, pp. 531–536, Apr. 1999.

[28] S. Bastonero, G. P. Bava, G. Chiaolò Piat, P. Debernardi, R. Orta, and R. Tascone, "Spontaneous emission evaluation in a photonic bandgap microcavity," *Opt. Quant. Electron.*, vol. 31, pp. 857–876, Oct. 1999.

[29] E.Özbay and B. Temelkuran, "Reflection properties and defect formation in photonic crystals," *Appl. Phys. Lett.*, vol. 69, pp. 743–745, Aug. 1996.

Fabrizio Frezza (S'87–M'90–SM'95) received the Laurea degree *cum laude* in electronic engineering and the doctorate degree in applied electromagnetics from "La Sapienza" University of Rome, Italy, in 1986 and 1991, respectively.

In 1986, he joined the Electronic Engineering Department of La Sapienza University, where he was Researcher from 1990 to 1998, a temporary Professor of Electromagnetics from 1994 to 1998, and an Associate Professor since 1998. His main research interests include guiding structures, antennas and resonators for microwaves and millimeter waves, numerical methods, scattering, optical propagation, plasma heating, and anisotropic media.

Dr. Frezza is a Member of Sigma Xi, of the Electrical and Electronic Italian Association (AEI), of Italian Society of Optics and Photonics (SIOF), of the Italian Society for Industrial and Applied Mathematics (SIMAI), and of Italian Society of Aeronautics and Astronautics (AIDAA).

Lara Pajewski received the Laurea degree (*cum laude*) in electronic engineering in 2000 from "Roma Tre" University of Rome, Italy.

In 2000, she joined the Department of Electronic Engineering, "La Sapienza" University of Rome, where she is presently a Ph.D. student in Applied Electromagnetics. Her main research interests are in electromagnetic analysis of periodic structures, scattering problems and numerical methods.

Giuseppe Schettini (S'82–M'96) received the Laurea degree (*cum laude*) in electronic engineering, the Ph. D. degree in applied electromagnetics, and the Laurea degree (*cum laude*) in physics from "La Sapienza" University of Rome, Rome, Italy, in 1986, 1991, and 1995, respectively.

In 1988, he joined the Italian Energy and Environment Agency (ENEA), where he was initially involved with free electron generators of millimeter waves and then on microwave components and antennas for the heating of thermonuclear plasmas. In 1992 he joined La Sapienza University as Researcher of electromagnetics. From 1995 to 1998, he was a temporary Professor of electromagnetics. Since 1998, he has been Associate Professor of antennas and of microwaves at the Roma Tre University of Rome, Rome, Italy. His research interests include scattering from cylindrical structures, ferrite resonators, electromagnetic analysis of diffractive optics, numerical methods and antennas.